

PACS numbers: 42.65.Es; 42.65.Re
DOI: 10.1070/QE2010v040n04ABEH014231

Spectrum of a pulse compressed in SBS in CCl_4 to nanosecond and subnanosecond durations

A.I. Erokhin, S.N. Datsenko, E.V. Loginov

***Abstract*. The change in the spectral shape and the Stokes frequency shift of radiation compressed in SBS is studied experimentally as a function of the incident laser pulse intensity. It is shown that when the duration of the reflected laser pulse is reduced down to the subnanosecond one, its spectrum is monotonically displaced with increasing the pump intensity, which leads to a decrease in the Stokes shift. Then, the spectrum splits and acquires a double-humped shape, which is explained by the presence of phase modulation in the vicinity of the SBS resonance.**

Keywords: *SBS, pulse compression, spectrum structure.*

1. Introduction

The problem of the spectral line shape produced in SBS is still open to discussion [1 – 4]. This is explained by a number of reasons.

First, the SBS line is rather narrow and its shape is difficult to study with the help of standard spectral devices such as a Fabry – Perot interferometer (even in such a substance as CCl_4, the linewidth is less than 3×10^{-3} cm^{-1}).

Second, in experiments with focused laser pulses [5], single-mode fibres [2], SBS amplifiers [6], or four-wave spectroscopy [7, 8], the laser radiation intensities required to obtain SBS or to study its line shape can differ by many order of magnitude and hence, it is difficult to compare the results obtained under different conditions.

The third factor, which may lead to the spectral shape deformation, can be the result of the feedback [4]. The feedback here means the formation of SBS resonators (see, for example, [9]), whose reflecting elements, due to giant gains, can be the cell surfaces or simply scattering dust.

Fourth, the SBS spectrum has a stochastic nature of this process, i.e. information on the SBS line shape, as in the case of SRS, requires several pulses to be formed [1, 10]. Therefore, to avoid hardware smoothing of the spectral peculiarities, it is necessary either to stabilise the excitation laser radiation frequency or to measure the spectral distribution in each pulse and only then to integrate it by selecting the laser line as a reference.

Pulse compression in SBS is a particular area in the SBS research because the process is fundamentally nonstationary [11, 12]. The Stokes pulse duration significantly decreases, which, according to the uncertainty principle, leads to the spectral broadening making it possible to study the spectral distribution with the help of a Fabry – Perot interferometer. Pulse shortening excludes the possibility of the feedback appearance, which does not have time to develop during the Stokes pulse formation. The discrepancies caused by the use of different schemes and thus by different laser intensities are also eliminated because use is made of megawatt laser pulses focused in a certain way to perform efficient compression. The problems associated with the statistics, in other words, with the reproducibility of the Stokes spectrum from pulse to pulse during compression, still remain open to question.

Previously, the spectrum of a pulse compressed in SBS was experimentally measured in papers [13, 14] with the help of a scanning interferometer. The obtained spectra were averaged over several pulses and the authors were interested in their half-widths.

In this paper, we study experimentally the SBS spectra during the compression of pulses of different durations at various pump powers as well as the self-phase modulation processes caused by the SBS nonlinearity.

2. First compression stage

The basic optical scheme of the experimental setup is presented in Fig. 1. The pulse was compressed with the help of SBS down to nanosecond durations by using two methods: the one-cell method, by using a SBS generator; and the two-cell method, by using the scheme with a SBS generator and a SBS amplifier (similarly to papers [13, 15]). A pulse (amplified up to 50 – 100 mJ) from a 1.055-μm single-mode, single-frequency, Q-switched Nd : glass laser propagated through optical polarisation Faraday isolator (*1*) whose magnetic field was formed by a system of permanent magnets. Then, the output pulse was broadened by collimator (*2*) up to 1.5 – 2 cm in diameter and focused by long-focus lens (*3*) in the vicinity of the output end of 2-m-long cell (*4*) filled with CCl_4. In one case, the focus was inside the cell and in the other – outside the cell (depending on the method employed).

Consider first the scheme with a generator, i.e. the case when the laser beam was focused inside the cell at a distance of ~ 30 cm from the output window. A phase-conjugated

A.I. Erokhin, S.N. Datsenko, E.V. Loginov P.N. Lebedev Physics Institute, Russian Academy of Sciences, Leninsky prosp. 53, 119991 Moscow, Russia; e-mail: aerokhin@sci.lebedev.ru

Received 28 September 2009; revision received 2 March 2010
Kvantovaya Elektronika **40** (4) 335 – 340 (2010)
Translated by I.A. Ulitkin

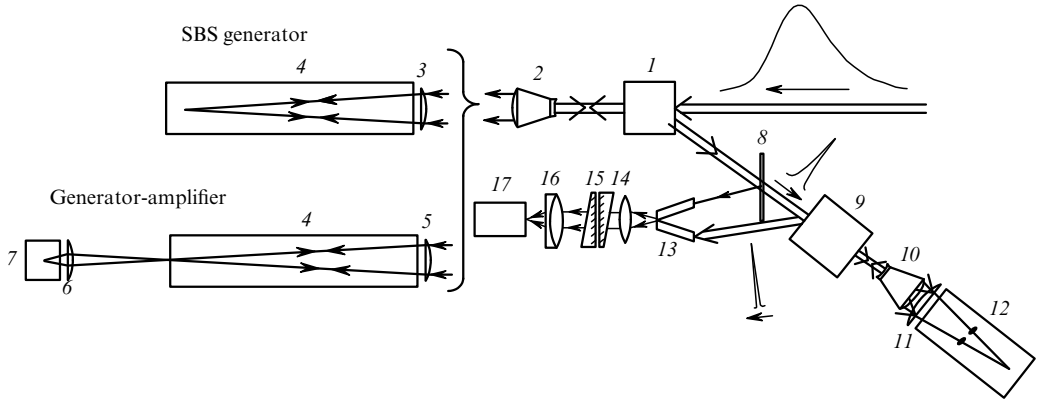

Figure 1. Basic scheme of the experimental setup: (*1*) optical Faraday isolator on permanent magnets; (*2*) fourfold collimator; (*3*, *5*) long-focus lenses; (*4*) two-meter cell of the first SBS compressor (filled with CCl_4); (*6*, *11*) focusing lenses; (*7*) thermostatically controlled cell with hexane; (*8*) plane-parallel plate; (*9*) polarisation decoupling based on Fresnel rhomb; (*10*) twofold collimator; (*12*) 70-cm cell with CCl_4 for recompression; (*13*) glass fibres; (*14*) reflecting lens; (*15*) Fabry–Perot interferometer; (*16*) objective; (*17*) CCD camera.

pulse reflected backward and compressed during SBS was coupled out with the help of polarisation isolator (*1*). Oscillograms of incident (Fig. 2a) and compressed (Fig. 2b, a) pulses were measured with a FK-15 photocell on the C7-19 oscilloscope. One can see from Fig. 2 that the bell-shaped laser pulse with the FWHM of 25 ns was converted during compression in a short pulse with a subnanosecond leading edge and a more sloping trailing edge. Its pulse duration varied from 1.3 to 1.7 ns depending on the pump level. Simultaneously with the temporal shape of the pulse, we detected the spectrum of reflected radiation (by using the method described in [16]). For this purpose, the beams of pump radiation and of light backscattered in SBS were separately coupled into glass fibres (*13*) with a rectangular cross section. The fibres were placed at a small angle to each other and their dull output ends touched one of the faces. Radiation scattered by the faces was collected by lens (*14*), transmitted through Fabry–Perot interferometer (*15*) with a 15-cm baselength, and imaged by objective (*16*) onto the LCL-902C CCD matrix so that the pump and SBS spectra were registered by different parts of the matrix. The dynamic range of the device relative to the intensity exceeded 200. The digitised interferograms were processed by a PC. Then, to determine the spectrum $I(\nu_{st})$, the interferogram centre and average energy densities were found; next, the argument was reduced to the linear dependence of the Stokes shift frequency $I(r^2)$. After it, the argument was shifted by a value corresponding to one of the pump distribution maxima as well as its normalisation.

Figure 3 presents the results of processing of the experimental data. The spectral shape of Stokes radiation was reproduced from pulse to pulse and only the position of the maximum varied in the range of ~ 100 MHz. The probability density of finding the spectrum maximum in this spectral range, determined by 50 measurements, is shown by curve (*1*). It has a double-humped shape and the peaks correspond to the components of the fine SBS structure obtained in CCl_4 under completely different experimental conditions [1]. If we consider the Stokes spectrum even in a single pulse, we neither find the fine structure not its presence in the averaged spectrum [see curve (*2*)]. In our opinion, this can be explained as follows. Obviously, already at the initial stage, the high-power hypersound frequency generated near the focus is related

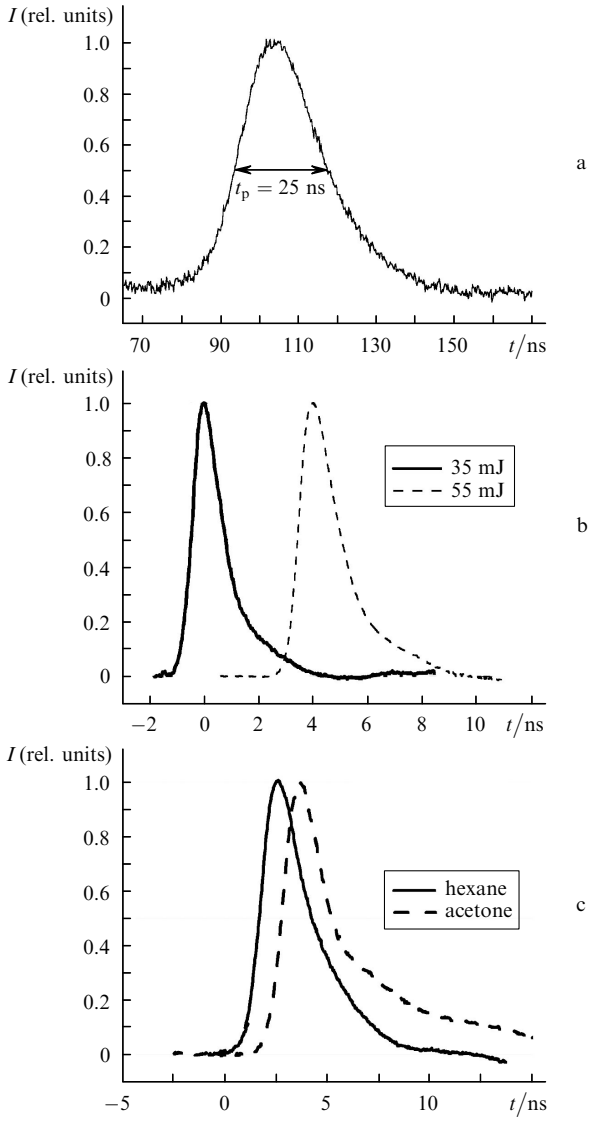

Figure 2. Oscillograms of an incident pulse (a) and pulse compressed in SBS at the initial stage of emission (b, c) in the case of generation at different levels of the pump excess over the threshold and $W = 35$ and 55 mJ (b) and upon amplifying seed signals generated in hexane (solid curve) or acetone (dashed curve) with a Stokes shift 2860 and 2990 MHz, respectively (c).

with a high probability to one of the doublet lines found in [1]. During the pulse compression which occupies most of the interaction region, the initial narrowband Stokes signal with a corresponding frequency shift is compressed in time, remaining Fourier transform limited. The spectral distribution of this signal is given by the expression $I(\omega) \propto |\int \sqrt{I(t)} \exp(i\omega t)dt|^2$, and the maximum corresponds to the narrowband seed frequency. Curve (*3*) was obtained from this expression, taking into account the temporal shape $I(t)$ of the compressed pulse. Comparison of this curve with integral spectrum (*2*) shows that we deal here with an insignificant phase modulation expanding the spectrum to the Stokes side. The phase modulation can be estimated from the expression for the field amplitude exponentially amplified with the increment $gI(t)L$ near the resonance line with a relative detuning from the resonance by $\delta = (\Omega_S - \Omega_{MB})/\Gamma$ [g, Ω_S, Ω_{MB}, Γ are the gain, Stokes shift, resonance Mandel'shtam – Brillouin (MB) frequency, and the line half-width, respectively]:

$$e_S(\delta) \propto \exp \frac{gIL}{1 - i\delta}. \quad (1)$$

Assuming that $I(t)$ has a smooth bell-like shape with a characteristic time t_p, we will estimate the spectrum broadening from the expression

$$\Delta\bar{\omega}_S \propto \frac{gIL}{t_p} \frac{\delta}{1 + \delta^2}.$$

This estimate gives the broadening ~ 100 MHz at $gIL = 25$, $\delta \sim 0.5$ and $t_p \sim 12$ ns.

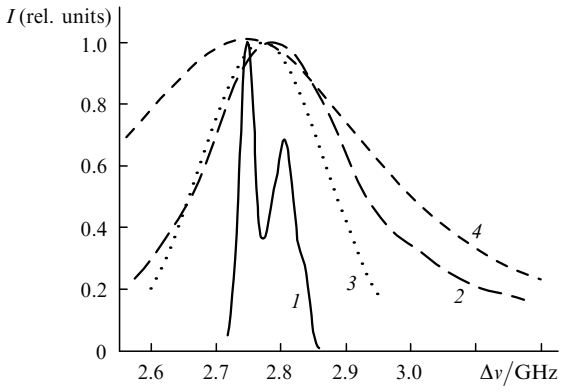

Figure 3. Spectral characteristics of Stokes radiation at the first stage of pulse compression obtained during generation; (*1*) probability of the position of the spectral distribution maximum; (*2*) spectral distribution of Stokes radiation averaged over 50 pulses; (*3*) spectral model taking into account only the amplitude modulation of the signal; (*4*) line spectrum of spontaneous scattering in CCl_4.

The spectrum of the pulse compressed during SBS at this compression stage (from 30 to 2 ns) is confined inside the spontaneous scattering line (*4*) taken from paper [7]. This spectrum detected in each pulse contains information on the structure typical of the stationary SBS, and its shape only slightly differs from the Fourier spectrum of a transform limited pulse.

It is known (see, for example, [17]) that the SBS compression of pulses in the generator regime is characterised by noticeable energy fluctuations of the compressed pulse. This seems to be caused by the instability of the Stokes frequency shift. To make the SBS compression of the pulse more stable, we used a two-cell compression scheme (see Fig. 1). An identical scheme was proposed for phase conjugation of high-power laser pulses [6], and later was used for pulse compression in paper [15]. This scheme can make use of the cells with the same substance. In our case, the generator cells were filled with the substances whose Stokes shifts were close to the resonance frequency of the amplifier. When the working substance was hexane or acetone, the compressed pulse duration was virtually the same (Fig. 2c) and amounted to the FWHM of ~ 2.5 ns. One can see from this figure that in one of the cases we deal with the pulse trailing edge pulling, which can be explained by the presence of radiation absorption in acetone, ~ 0.05 cm^{-1}. Then, we used a cell with hexane placed into a thermostat as a generator. The thermostat temperature increased from 15 to 35 °C; in this case, the Stokes shift of the seed signal changed so that we could choose any segment of the central spectral part of the SBS-amplifier filled with CCl_4, which operated at room temperature (20 ± 1 °C).

Figure 4 presents the dependence of the gain R_{comp} on the frequency of the seed Stokes signal received from a cell with hexane. We will determine R_{comp} as a peak pulse power during SBS, normalised to the peak power of the pump pulse. In our experiments, this quantity is noticeably larger than unity. One can see that the SBS compressor operates stably and efficiently in the region of the seed Stokes wave frequency (2.7 – 2.8 GHz). In the experiment, this corresponds to the hexane temperature 25 ± 3 °C, which was used in further tests.

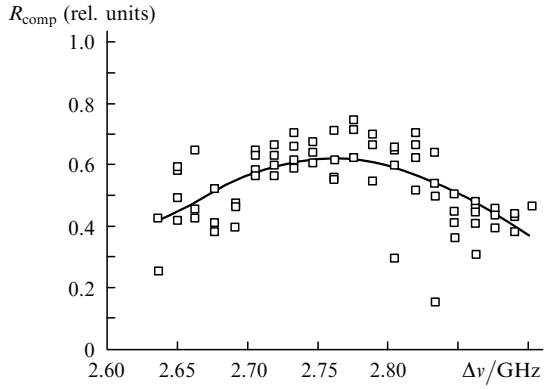

Figure 4. Dependence of the SBS conversion efficiency at the first stage of pulse compression on the seed radiation frequency; squares are the experiment and the curve is the approximation by Gaussian distribution.

3. Pulse recompression

To convert the energy of a high-power laser pulse with duration of tens of nanoseconds to the subnanosecond range, double SBS compression is required. This is caused by a number of reasons. First, energy is effectively converted into a Stokes wave only at the compression coefficients no more than 10. Second, the power required for SBS generation grows exponentially only when the

pump pulse duration approaches $\tau = 1/\Gamma$ [18] and the competing processes of SRS type [19] are brought to the fore. Thus, to obtain a pulse with duration smaller than τ, we first compressed it down to duration of several τ and then recompressed it.

The optical scheme of the recompression stage is shown in the right-hand side of Fig. 1. The frequency- and intensity-stabilised laser pulse compressed down to ~ 2.5 ns in the two-cell scheme was coupled out during the backward pass through Faraday isolator (*1*). Then, the pulse propagated through beamsplitting plate (*8*) and polarisation decoupling based on Fresnel rhomb (*9*). After it, the beam responsible for pumping was broadened by collimator (*10*) up to diameter ~ 1 cm and focused into the part (farthest from the input window) of the 70-cm cell also filled with CCl_4. Backward reflected Stokes radiation was deflected by polarisation decoupling (*9*) into a system registering the spectrum and the temporal shape. The latter was detected with the FK-15 photocell connected to the C7-19 oscilloscope. Figures 5a, b show the oscillograms of the compressed pulses. Figure 5c presents for comparison the instrument function of the receiver, obtained with the help of a subpicosecond laser pulse. The compressed pulse duration can be estimated, assuming that the square of the duration on the oscillogram with respect to the half-height is obtained from the sum of the squares of the duration of the pulse itself and the width of the instrument function. This estimate is rigorously valid only for Gaussian pulses but gives satisfactory results also for other smooth pulses. Bearing this in mind we obtain that the compressed pulse duration in Fig. 5a is $t_p = 400 \pm 50$ ps. In the case, when the pump intensity exceeded the SBS threshold by several times, the compressed pulse duration (Fig. 5b) was less than 300 ps, and the above described method for taking into account the instrument function proved unfit because the errors in determining t_p were comparable with the result.

The spectral distributions of the pump radiation and Stokes signal (Fig. 6) were obtained by using a Fabry–Perot interferometer with a 7.5-cm baselength; as a result, the SBS spectrum in CCl_4 (where $\Delta\nu \sim 2.75$ GHz) was observed only in the case of double overlap of the orders. However, because the fields of the Stokes signal (the upper part of the spectrogram) and pump (the lower part) are separated this overlap did not noticeably affect the quality of the measured spectra. In the vicinity of the SBS observation threshold (Fig. 6a), the compressed pulse spectrum was of a bell-like shape. When the pump level largely exceeded the threshold, the Stokes spectrum strongly broadened and became two-humped (Fig. 6b).

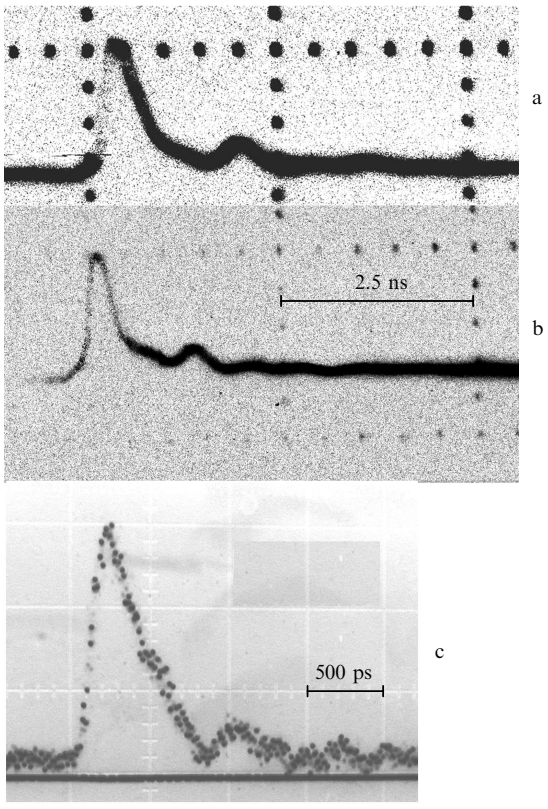

Figure 5. Oscillograms of pulses compressed in SBS down to subnanosecond durations at pump levels exceeding the lasing threshold by 1.5–2 times (a) and five times (b); (c) is the instrument function of the detecting FK-15 photocell.

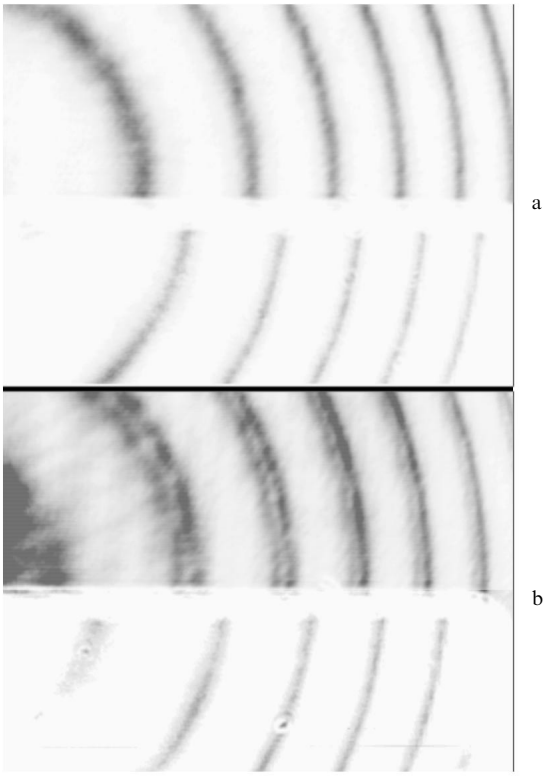

Figure 6. Spectra of Stokes radiation compresses down to subnanosecond durations in the vicinity of the lasing threshold (a) and in the case of fivefold excess over the threshold (b). Upper part of the spectrograms corresponds to Stokes radiation and the lower – to pump.

An increase in the pump from the threshold value to the level, exceeding the threshold by more than eight times, allowed us to follow the behaviour of the spectrum of radiation compressed down to subnanosecond duration. For clearness, the peak value of the spectral distribution in each case was normalised to unity. The data array of the spectral values obtained in this way was represented in the form of a three-dimensional plot whose third coordinate is the pump energy W. The spectral dependence of the array of

the experimental points $I(\Delta v, W)$ shown in Fig. 7 was plotted using the MathLab software package. One should not be surprised by the fact the the pump energy plotted on one of the axes does not exceed 20 mJ because it is necessary to remember that the pump pulse duration is ~ 2.5 ns and the intensity in the lens focus for these energies is close to the intensity at which an optical breakdown in a liquid is observed. Figure 7 (because of the averaging inherent in MathLab) shows only the general tendency of a change in the SBS spectrum in the nonstationary case up to almost a tenfold excess over the threshold. Let us describe these experimental results in detail.

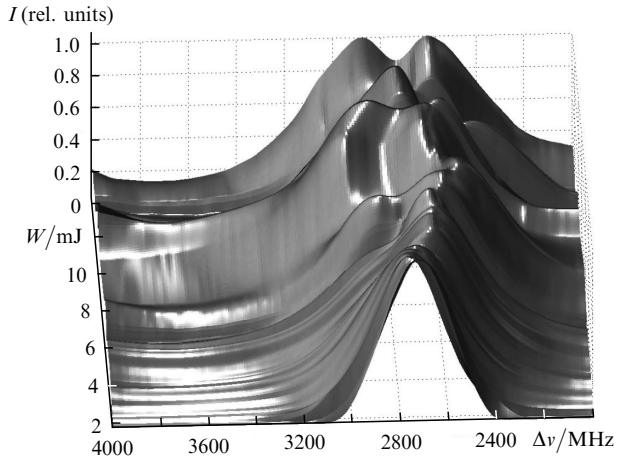

Figure 7. Spectral intensity distribution of subnanosecond Stokes radiation normalised to unity and its dependence on the pump energy of duration 2.5 ns.

Near the threshold, the Stokes spectrum has a Gaussian shape with the half-width of 335 ± 10 MHz. This is deliberately larger than the stationary value estimated $\Delta v_{sp}/\sqrt{G} \sim 100$ MHz (for $G = gIL \sim 25$), where Δv_{sp} is the width of the spontaneous Brillouin line at FWHM and G is the gain increment. Note that the position of the spectrum maximum at identical pump intensities is stable with an accuracy up to 20 MHz, i.e. radiation whose spectrum is in the vicinity of the SBS resonance centre develops from spontaneous noises. While increasing the pump intensity up to threefold access over the threshold, we observed a monotonic displacement of the Stokes line maximum approximately by 150 MHz, the line shape remaining Gaussian in this case.

When the threshold is exceeded by 3–3.5 times, the SBS spectrum is not uniquely defined by the position of the maximum and is far from Gaussian. If the maximum of the spectrum is displaced from the SBS resonance (which occurs most often), we observe, in the direction to the resonance, a sloping line wing with a weakly pronounced maximum in those case when this wing is rather intense. In the case of a four–eightfold excess over the threshold, the SBS spectrum stably has a doublet shape. The distance between the doublet maxima remains constant (300 ± 20 MHz) and the entire linewidth (FWHM) is ~ 800 MHz, i.e. noticeably exceeds the linewidth of spontaneous Brillouin scattering (~ 530 MHz). The doublet maxima are located symmetrically with respect to the line centre. The position of the maxima changes by 100–150 MHz, i.e. if to measure the SBS spectrum integrally (per several pulses), the doublet will be absent in the spectrum (obviously, this is the case in paper [14]). Note that the observed doublet consists of broad lines and does not contain narrowband components, which would indicate the presence of not very intense but time stretched tail of the Stokes pulse.

4. Discussion of the results. Conclusions

Time integrated measurements of the Stokes spectrum during the SBS compression of a laser pulse from 25 to 1.5–2.5 ns have shown that at this stage SBS spectrum is smooth, amplitude modulated and transform limited. The maximum of the spectral distribution in each realisation is found for the Stokes shift eigenfrequency at which the SBS compression develops. Statistics of the position of the maxima coincides with the SBS spectrum structure we found previously.

Thus, it has been determined experimentally that the phase modulation during the SBS compression of a pulse is not observed in the spectrum until the Stokes pulse duration is smaller than the lifetime of hypersound phonons ($t_p > \tau$). This is explained by the fact that amplification of Stokes radiation will be virtually uniform with respect to the frequency in the vicinity of the Brillouin line peak.

At the next compression stage (from 2.5 to 0.5–0.3 ns), radiation experiences phase modulation. This is first manifested in a decrease in the Stokes shift near the SBS observation threshold. When the pump intensity is increased, the spectrum becomes unstable, broadening in the direction of the Brillouin resonance in the form of a wing. The further increase in the pump intensity leads to spectrum stabilisation; it becomes two-humped, symmetric with respect to the position of the SBS resonance of the liquid under study (in this case, CCl_4).

When the pulse is shortened down to the values smaller than τ, radiation spectrally broadens and the amplification process becomes thus frequency inhomogeneous. Moreover, because of the asymmetry of the SBS resonance [20], the spectral part of Stokes radiation with the smallest frequency shift will experience the largest amplification. At the initial stage, this will result in a decrease in the Stokes shift of the line. With a stronger interaction, most of the energy already at the pulse onset will be on the anti-Stokes side from the resonance with a characteristic displacement by $\Delta\Omega$, which is $\sim 2\pi \cdot 150$ MHz in our case (see Fig. 7). In this case, for time t so that $t\Delta\Omega \sim \pi$, the phase of the acoustic wave will be shifted, leading to its suppression; as a result, the anti-Stokes part of the line will be suppressed and its Stokes part will be generated, accompanied by the pump saturation. With exceeding manifold the SBS threshold, the process can be repeated.

The Brillouin line asymmetry depends on the ratio of its half-width to the Stokes shift quantity. This ratio (for CCl_4 it is ~ 0.1) determines the phase-modulation dynamics. The quantity of splitting should be comparable with the linewidth, which is observed in the experiment. Present investigations of the phase-modulation properties during the SBS compression can form the basis for selecting the theoretical model of the process; the quantitative description of the phase-modulation phenomenon in SBS is a separate problem and will be performed elsewhere.

Acknowledgements. The authors thank Yu.V. Mityagin for placing at our disposal the elements of the recording devices

and V.I. Erokhina and A.V. Masalov for the support of the present work.

References

1. Erokhin A.I., Oleinikov V.V., Putilin A.V. *Pis'ma Zh. Eksp. Teor. Fiz.*, **61**, 873 (1995).
2. Kovalev V.I., Harrison R.G. *Phys. Rev. Lett.*, **85**, 1879 (2000).
3. Stépien L., Randoux S., Zemmouri J. *Phys. Rev. A*, **65**, 053812-1 (2002).
4. Erokhin A.I., Efimkov V.F., Zubarev I.G., et al. *Kvantovaya Electron.*, **26**, 144 (1999) [*Quantum Electron.*, **29**, 144 (1999)].
5. Dane C. B., Hackel L.A., in *'Phase Conjugate Laser Optics'* (New York: John Wiley and Sons, 2004) Chap. 5.
6. Basov N., Zubarev I. *Appl. Phys. Lett.*, **20**, 261 (1979).
7. Erokhin A.I., Kovalev V.I., Faizullov F.S. *Kvantovaya Electron.*, **13**, 1328 (1986) [*Sov. J. Quantum Electron.*, **16**, 872 (1986)].
8. Faris G.W., Dyer, M. J., Hickman A.P. *Opt. Lett.*, **17**, 1049 (1992).
9. Odintsov V.I., Rogachev L.F. *Pis'ma Zh. Eksp. Teor. Fiz.*, **36**, 281 (1982).
10. Mc Person D.S., Swanson R.S., Carlsten J.I. *Phys. Rev. A*, **32**, 3487 (1989).
11. Hon D.T. *Opt. Lett.*, **5**, 516 (1980).
12. Gorbunov V.A., Ivanov V.B., Papernyi S.B., et al. *Izv. Akad. Nauk SSSR. Ser. Fiz.*, **48**, 1580 (1984).
13. Schiemann S., Hogervorst W., Ubachs W. *IEEE J. Quantum Electron.*, **34**, 407 (1998).
14. Kmetik V., Yoshida H., Fujita H., et. al. *Proc. SPIE Int. Soc. Opt. Ing.*, **3889**, 818 (2000).
15. Dane C.B., Newman W.A., Hackel L.A. *IEEE J. Quantum Electron.*, **30**, 1907 (1994).
16. Ragul'skii V.V. *Obrashchenie volnovogo fronta pri vynuzhdennom rasseyanii sveta* (Phase Conjugation upon Stimulated Light Scattering) (Moscow: Nauka, 1990).
17. Velchev I., Ubachs W. *Phys. Rev. A*, **71**, 043810 (2005).
18. Hagenlocker E.E., Minck R.W., Rado W.G. *Phys. Rev.*, **154**, 226 (1967).
19. Buzyalis R.R., Gidrauskas V.V., Dement'ev A.S., et al. *Kvantovaya Electron.*, **14**, 2266 (1987) [*Sov. J. Quantum Electron.*, **17**, 1444 (1987)].
20. Fabelinskii I.L. *Molecular Scattering of Light* (New York: Plenum Press, 1968; Moscow: Nauka, 1965).